



EUROPEAN ORGANIZATION FOR NUCLEAR RESEARCH

MEASUREMENT OF HADRON AZIMUTHAL DISTRIBUTIONS IN DEEP

INELASTIC MUON PROTON SCATTERING

CERN-EP/86-169  
3 November 1986

The European Muon Collaboration

Aachen<sup>1</sup>, CERN<sup>2</sup>, DESY (Hamburg)<sup>3</sup>, Freiburg<sup>4</sup>, Hamburg (University)<sup>5</sup>,  
Kiel<sup>6</sup>, LAL (Orsay)<sup>7</sup>, Lancaster<sup>8</sup>, LAPP (Annecy)<sup>9</sup>, Liverpool<sup>10</sup>, Marseille<sup>11</sup>,  
Mons<sup>12</sup>, MPI (München)<sup>13</sup>, Oxford<sup>14</sup>, RAL (Chilton)<sup>15</sup>, Sheffield<sup>16</sup>,  
Torino<sup>17</sup>, Uppsala<sup>18</sup>, Warsaw<sup>19</sup>, Wuppertal<sup>20</sup>.

M. Arneodo<sup>17</sup>, A. Arvidson<sup>18</sup>, J.J. Aubert<sup>11</sup>, B. Badelek<sup>19a</sup>, J. Beaufays<sup>2</sup>,  
C.P. Bee<sup>8b</sup>, C. Benchouk<sup>11</sup>, G. Berghoff<sup>1</sup>, I. Bird<sup>8c</sup>, D. Blum<sup>7</sup>, E. Böhm<sup>6</sup>,  
X. de Bouard<sup>9</sup>, F.W. Brasse<sup>3</sup>, H. Braun<sup>20</sup>, C. Broll<sup>9+</sup>, S. Brown<sup>10d</sup>,  
H. Brück<sup>20e</sup>, H. Calen<sup>18</sup>, J.S. Chima<sup>15f</sup>, J. Ciborowski<sup>19a</sup>, R. Clifft<sup>15</sup>,  
G. Coignet<sup>9</sup>, F. Combley<sup>16</sup>, J. Conrad<sup>14</sup>, J. Coughlan<sup>8E</sup>, G. D'Agostini<sup>11</sup>,  
S. Dahlgren<sup>18</sup>, F. Dengler<sup>13</sup>, I. Derado<sup>13</sup>, T. Dreyer<sup>4</sup>, J. Drees<sup>20</sup>, M. Düren<sup>1</sup>,  
V. Eckardt<sup>13</sup>, A. Edwards<sup>20h</sup>, M. Edwards<sup>15</sup>, T. Ernst<sup>4</sup>, G. Eszes<sup>9i</sup>,  
J. Favier<sup>9</sup>, M.I. Ferrero<sup>17</sup>, J. Figiel<sup>5j</sup>, W. Flauger<sup>3</sup>, J. Foster<sup>16k</sup>,  
E. Gabathuler<sup>10</sup>, J. Gajewski<sup>5</sup>, R. Gamet<sup>10</sup>, J. Gayler<sup>3</sup>, N. Geddes<sup>14g</sup>,  
P. Grafström<sup>18</sup>, F. Grard<sup>12</sup>, J. Haas<sup>4</sup>, E. Hagberg<sup>18</sup>, F.J. Hasert<sup>11</sup>,  
P. Hayman<sup>10</sup>, P. Heusse<sup>7</sup>, M. Jaffré<sup>7</sup>, A. Jacholkowska<sup>2</sup>, F. Janata<sup>5</sup>,  
G. Jancso<sup>13i</sup>, A.S. Johnson<sup>14m</sup>, E.M. Kabuss<sup>4</sup>, G. Kellner<sup>2</sup>, V. Korbel<sup>3</sup>,  
J. Krüger<sup>20e</sup>, S. Kullander<sup>18</sup>, U. Landgraf<sup>4</sup>, D. Lanske<sup>1</sup>, J. Loken<sup>14</sup>,  
K. Long<sup>14n</sup>, M. Maire<sup>9</sup>, P. Malecki<sup>13</sup>, A. Manz<sup>13</sup>, S. Maselli<sup>13</sup>, W. Mohr<sup>4</sup>,  
F. Montanet<sup>11</sup>, H.E. Montgomery<sup>20</sup>, E. Nagy<sup>9i</sup>, J. Nassalski<sup>19p</sup>,  
P.R. Norton<sup>15</sup>, F.G. Oakham<sup>15q</sup>, A.M. Osborne<sup>2</sup>, C. Pascaud<sup>7</sup>, N. Pavel<sup>20</sup>,  
B. Pawlik<sup>13</sup>, P. Payre<sup>11</sup>, C. Peroni<sup>17</sup>, H. Peschel<sup>20</sup>, H. Pessard<sup>9</sup>,  
J. Pettingale<sup>10</sup>, B. Pietrzyk<sup>11</sup>, B. Pönsgen<sup>5</sup>, M. Pötsch<sup>20</sup>, P. Renton<sup>14</sup>,  
P. Ribarics<sup>9i</sup>, K. Rith<sup>4c</sup>, E. Rondio<sup>19a</sup>, M. Scheer<sup>1</sup>, A. Sandacz<sup>19p</sup>,  
A. Schlagböhmer<sup>4</sup>, H. Schiemann<sup>5</sup>, N. Schmitz<sup>13</sup>, M. Schneegans<sup>9</sup>, M. Scholz<sup>1</sup>,  
T. Schröder<sup>4</sup>, K. Schultze<sup>1</sup>, T. Sloan<sup>8</sup>, H.E. Stier<sup>4</sup>, M. Studt<sup>5</sup>,  
G.N. Taylor<sup>14</sup>, J.M. Thénard<sup>9</sup>, J.C. Thompson<sup>15</sup>, A. de la Torre<sup>5r</sup>, J. Toth<sup>9i</sup>,  
L. Urban<sup>1</sup>, L. Urban<sup>9i</sup>, W. Wallucks<sup>4</sup>, M. Whalley<sup>16s</sup>, S. Wheeler<sup>16</sup>,  
W.S.C. Williams<sup>14</sup>, S.J. Wimpenny<sup>10n</sup>, R. Windmolders<sup>12</sup>, G. Wolf<sup>13</sup>.

(Submitted to Zeits für Physik C)

Abstract

A study of the distribution of the azimuthal angle  $\phi$  of charged hadrons in deep inelastic  $\mu$ -p scattering is presented. The dependence of the moments of this distribution on the Feynman  $x$  variable and the momentum transverse to the virtual photon indicates that non-zero moments arise mainly from the effects of the intrinsic  $K_T$  of the struck quark with  $\langle K_T^2 \rangle \gtrsim (0.44 \text{ GeV})^2$ , and to a lesser extent from QCD processes. No significant variation with  $Q^2$  or  $W^2$  is observed.

For footnotes see next page.

Addresses

- 1) III. Physikalisches Inst. A, Physikzentrum, Aachen, Germany.
  - 2) CERN, Geneva, Switzerland.
  - 3) DESY, Hamburg, Germany.
  - 4) Fakultät für Physik, Universität Freiburg, Germany.
  - 5) II Institut für Experimentalphysik, Universität Hamburg, Germany.
  - 6) II Institut für Kernphysik, Universität Kiel, Germany.
  - 7) Laboratoire de l'Accélérateur Linéaire, Université de Paris-Sud, Orsay, France.
  - 8) Department of Physics, University of Lancaster, England.
  - 9) Laboratoire d'Annecy de Physique des Particules, IN2P3, Annecy-le-Vieux, France.
  - 10) Department of Physics, University of Liverpool, England.
  - 11) Centre de Physique des Particules, Faculté des Sciences de Luminy, Marseille, France.
  - 12) Faculté des Sciences, Université de L'Etat à Mons, Belgium.
  - 13) Max-Planck-Institut für Physik und Astrophysik, München, Germany.
  - 14) Nuclear Physics Laboratory, University of Oxford, England.
  - 15) Rutherford and Appleton Laboratory, Chilton, Didcot, England.
  - 16) Department of Physics, University of Sheffield, England.
  - 17) Istituto di Fisica, Università di Torino, Italy.
  - 18) Gustav Werners Institut, University of Uppsala, Sweden.
  - 19) Physics Institute, University of Warsaw, and Institute for Nuclear Studies, Warsaw, Poland.
  - 20) Fachbereich Physik, Universität Wuppertal, Germany.
- 
- a) University of Warsaw, Poland.
  - b) Now at University of Liverpool, England.
  - c) Now at MPI für Kernphysik, Heidelberg, Germany.
  - d) Now at TESA S.A., Renens, Switzerland.
  - e) Now at DESY, Hamburg, W. Germany.
  - f) Now at British Telecom, Ipswich, England.
  - g) Now at RAL, Chilton, Didcot, England.
  - h) Now at Jet, Joint Undertaking, Abingdon, England.
  - i) Permanent address: Central Research Institute for Physics of the Hungarian Academy of Science, Budapest, Hungary.
  - j) Permanent address: Institute of Nuclear Physics, Krakow, Poland.
  - k) Now at University of Manchester, England.
  - l) Now at Krupp Atlas Elektronik GmbH, Bremen, Germany.
  - m) Now at SLAC, Stanford, California.
  - n) Now at CERN, Geneva, Switzerland.
  - o) Now at FNAL, Batavia, Illinois, U.S.A.
  - p) Institute for Nuclear Studies, Warsaw, Poland.
  - q) Now at NRC, Ottawa, Canada.
  - r) Now at Universidad Nacional, Mar del Plata, Argentina.
  - s) Now at University of Durham, England.
  - +) Deceased.

## Introduction

It was suggested several years ago by Georgi and Politzer [1] that hadron asymmetries around the current axis in deep inelastic scattering could provide a test of perturbative QCD predictions. In contrast Cahn [2] showed that non-perturbative properties such as  $K_T$ , the intrinsic transverse momentum of the struck quark inside the nucleon can also induce such asymmetries. In addition recent work by Berger [3] has shown that higher twist effects should also be considered. Unfortunately, the fundamental parton processes described by these models are obscured by the fragmentation of partons into hadrons. Fragmentation was taken into account in the model of König and Kroll [4] in which the effects of  $K_T$  and lowest order QCD were studied. Comparing the results of König and Kroll to an earlier EMC measurement [5] it was concluded that the most important factor was  $K_T$  which effectively masked the QCD effects. However, to fit the data a value of  $K_T \sim 0.7$  GeV was required which seems unphysically large given the effective radius of the proton. These results [5] were however limited to the forward CMS hemisphere and need to be completed by a measurement that includes the backward hemisphere. Such a measurement is presented here for the first time in deep inelastic muon scattering and shows that the asymmetries have a very different character in the backward region. These results are again compared to the model of König and Kroll.

## Notation

The standard kinematic variables of deep inelastic scattering,  $Q^2$ ,  $\nu$ ,  $W^2$  and  $y$  have been used in the analysis. Here  $Q^2$  is the four momentum transfer squared and  $\nu$  the energy transfer to the virtual photon in the laboratory frame.  $W$  is the total energy in the centre of mass system (CMS) between the incoming proton and the virtual photon and hence of the final state hadrons and  $y = \nu/E_\mu$  where  $E_\mu$  is the energy of the incident muon.

The kinematics of the interaction are illustrated in fig. 1. The incoming muon emits a virtual photon which interacts with one of the partons in the proton. The incoming and outgoing muon lines, along with the virtual

photon direction define the lepton scattering plane. After the parton interacts with the virtual photon, it fragments forming the forward or current jet. The target remnants also fragment forming the backward or target jet. The incoming proton, the target and current jets and the intrinsic transverse momentum of the struck quark  $K_T$  all lie within the parton plane. The kinematics of the produced hadrons are measured in the CMS in which the x direction is along the virtual photon direction, the y axis is perpendicular to the x direction in the lepton scattering plane and towards the scattered muon and z is perpendicular to both to form a right handed system. The CMS transverse and longitudinal momenta of a hadron relative to the virtual photon are designated by  $p_T$  and  $p_L$ , respectively. The Feynman x variable is defined as  $x_F = 2p_L/W$ .

The angle  $\phi$  is the azimuthal angle of a hadron around the virtual photon direction with  $\phi = 0$  in the positive y direction. The moments of interest [5] namely  $\langle \cos\phi \rangle$ ,  $\langle \cos 2\phi \rangle$  and  $\langle \sin\phi \rangle$  were determined by fitting the observed normalised distribution to a function of the form

$$\frac{1}{N_\mu} \frac{dN^{h\pm}}{d\phi} = g(\phi) = A + B\cos\phi + C\cos 2\phi + D\sin\phi \quad (1)$$

The moment of a circular function  $m(\phi)$  is defined as

$$\langle m(\phi) \rangle = \frac{\int_0^{2\pi} g(\phi)m(\phi) d\phi}{\int_0^{2\pi} g(\phi) d\phi} \quad (2)$$

Thus the moments are  $\langle \cos\phi \rangle = B/2A$ ,  $\langle \cos 2\phi \rangle = C/2A$ ,  $\langle \sin\phi \rangle = D/2A$ . Note that with this definition the maximum physical value for the magnitude of these moments is 0.5. Each moment has a calculable kinematic dependence on y [1,2]. These are given by:

$$f_1(y) = \frac{(2-y)[1-y]^{1/2}}{1+(1-y)^2}, \quad f_2(y) = \frac{1-y}{1+(1-y)^2}, \quad f_3(y) = \frac{y[1-y]^{1/2}}{1+(1-y)^2} \quad (3)$$

for  $\langle \cos\phi \rangle$ ,  $\langle \cos 2\phi \rangle$  and  $\langle \sin\phi \rangle$  respectively. To remove this dependence each moment is divided by the mean of the appropriate function for the kinematic range selected.

### Theoretical Considerations

A non-zero  $\langle \cos\phi \rangle$  can arise simply from the intrinsic  $K_T$  of the struck quark (fig. 1). As the struck quark has a finite  $K_T$  it is possible to define a parton plane. It has been shown from the kinematics of the reaction [2] that the interaction probabilities between the quark and lepton are dependent on the relative orientation of the lepton and quark planes. This results in more hadrons being produced on the side opposite the scattered muon in the current jet, giving a negative  $\langle \cos\phi \rangle$  in the forward direction. As the target remnants must balance  $p_T$  there will be a positive  $\langle \cos\phi \rangle$  in the backward direction. Note that the relative magnitude of  $\langle \cos\phi \rangle$  in the forward and backward directions will depend on the details of the quark and di-quark fragmentation functions.

The emission of a hard gluon by the quark before or after the interaction can also give rise to a  $\phi$  asymmetry [1]. This arises because of asymmetries in the orientation of the hard gluon and scattered quark and differences in their fragmentation functions. Calculations by König and Kroll [4] indicate that this effect is sizeable above an  $x_F$  of about 0.2 but goes to zero as  $x_F$  approaches 1 as the quark and gluon become collinear. The effect is also strongly dependent on the  $p_T$  of the hadrons.

The  $\langle \cos\phi \rangle$  arising from higher twist effects [3] has been calculated and is expected to dominate at large positive  $x_F$ . Higher twist effects should contribute a large positive  $\langle \cos\phi \rangle$  in the  $x_F$  region from 0.5 to 1.0 with a magnitude similar to that produced by  $K_T$ . This contribution is assumed to add incoherently [7] to those of  $K_T$  and QCD discussed above.

### Data Analysis

The data were obtained using the M2 muon beam at the CERN SPS. Muons of energy 280 GeV were incident on a 1 m long liquid hydrogen target situated inside a streamer chamber which was itself located in a large vertex spectrometer magnet. The streamer chamber together with a system of drift and proportional chambers placed at wide angles were used to detect and measure the low and intermediate momentum hadrons produced in deep inelastic scattering. The scattered muons and fast forward hadrons were detected and measured in a forward spectrometer. The total system served to measure charged particles of momenta  $\gtrsim 0.2$  GeV with high efficiency, giving essentially  $4\pi$  coverage in the CMS. The details of both the vertex and forward spectrometers together with the analysis procedures are published elsewhere [8].

Events were selected by making kinematic cuts to avoid regions where the corrections for acceptance and radiative effects were large and rapidly varying. These cuts were  $Q^2 > 4 \text{ GeV}^2$ ,  $40 < W^2 < 450 \text{ GeV}^2$ ,  $\nu > 20 \text{ GeV}$  and  $y < 0.8$ . The  $y$  cut was particularly important in removing events with large radiative effects. The radiation of real photons produces a substantial non-zero  $\langle \cos\phi \rangle$ . To further reduce such effects events were excluded if the sum of the energies of all observed hadrons was less than 10% of the energy of the virtual photon,  $\nu$ . The number of events remaining after these cuts was 27,000.

About 50% of the hadrons in these events were identified by the apparatus. All other hadrons were assigned a pion mass except for positive hadrons having  $x_F(m_\pi) < -0.2$  and  $x_F(m_p) > -0.9$  which were assigned the proton mass. This assignment was based on a study using both the data and the Lund model which showed that  $> 90\%$  of all positive tracks in this region were protons [9]. For studies of  $\langle \cos\phi \rangle$  as a function of  $x_F$  an additional cut on all hadrons with  $p_T < 0.2 \text{ GeV}$  was applied to remove low  $p_T$  tracks in which  $\phi$  was poorly measured.

Acceptance corrections including radiative corrections were determined from a complete Monte Carlo simulation of the experiment. Deep inelastic scattering events were generated using the Lund String Model [10]. Secondary interactions of these hadrons and photon conversions in the target material were also produced. Hits were generated in all the detectors in such a way as to include the effects of the measured chamber and hodoscope efficiencies. Finally the simulated chamber and hodoscope data were passed through the analysis programme chain. The acceptance was then obtained from the ratio of the accepted hadrons to generated hadrons falling in any given bin. In this way corrections due to the apparatus and the analysis programmes were taken into account.

### Results

The  $\phi$  distributions of charged hadrons for several regions of  $x_F$  are shown in fig. 2 together with the results of fits of equation (1). The major effect observed was the variation of  $\langle \cos\phi \rangle / f_1(y)$  as a function of  $x_F$  as shown in fig. 3. Here one sees that at negative  $x_F$ ,  $\langle \cos\phi \rangle / f_1(y)$  is positive. The moment becomes negative at  $x_F \sim 0$  and falls below a value of  $-0.1$  for an  $x_F > 0.5$ . The data were checked for systematic effects by measuring  $\langle \cos\phi \rangle$  as a function of  $x_F$  in different spatial regions of the spectrometer. Variations in  $\langle \cos\phi \rangle$  induced in this manner were always found to be less than the statistical errors. The results of an earlier EMC measurement [5] in the positive  $x_F$  region are also given in fig. 3. These were obtained using a single magnet spectrometer system which had a substantially different acceptance from the apparatus used for the new data. The agreement between the two measurements is reasonable, supporting the above conclusion that systematic effects do not appear to be important.

The smooth curves in fig. 3 are the results of calculations made using the model of König and Kroll [4]. This model contains the effects of  $O(\alpha_s)$  corrections to the matrix element and of the intrinsic transverse momentum of the struck quark,  $K_T$ . The Lund string fragmentation model [10] is used

for the hadronisation of the partons. It can be seen that the predicted asymmetry arising from QCD alone (dashed curve) does not reproduce the large negative values of  $\langle \cos\phi \rangle$  in the forward hemisphere. Including the effect of  $K_T$  ( $\langle K_T^2 \rangle = (0.44 \text{ GeV})^2$ ) improves the agreement with the data including the observed positive values in the backward hemisphere. However, the absolute values in the forward direction are not well reproduced, nor is the rapid change in  $\langle \cos\phi \rangle$  around  $x_F \approx 0$ . Increasing  $K_T$  to  $\langle K_T^2 \rangle = (0.88 \text{ GeV})^2$  produces an asymmetry in the forward hemisphere which is still less than that observed. It should be noted that the possible effects of soft gluon radiation, the inclusion of which reproduces the transverse momentum properties of the hadrons in this experiment [11], are not included in the model. The model curves were calculated to a statistical precision of 0.02.

As the model of König and Kroll only includes corrections of  $O(\alpha_s)$ , higher twist effects must be considered independently. The data presented in fig. 3 show no indication that the  $\langle \cos\phi \rangle$  becomes more positive in the region of  $x_F$  from 0.5 to 1.0. Thus as with the results of earlier observations [12], there is no evidence for a higher twist contribution; however such a contribution cannot be ruled out.

The variation of  $\langle \cos\phi \rangle / f_1(y)$  as a function of  $p_T$  for different  $x_F$  regions is shown in fig. 4a. At small  $p_T$ , the values are consistent with zero in all  $x_F$  regions. For  $x_F > 0.15$  the absolute value of the moment increases as  $p_T$  increases. For  $x_F < -0.15$  the moment also increases in magnitude with  $p_T$  but this is of minimal statistical significance. A strong increase in  $|\langle \cos\phi \rangle|$  with  $p_T$  is expected if the moment arises from hard QCD effects [3]. An additional feature of the results shown in fig. 4a is that, at small values of positive  $x_F$ , there is a significant and slowly varying negative moment over a wide range of  $p_T$  values.

It is possible to enhance the fraction of events involving hard QCD processes by selecting events with a high  $p_T$  trigger particle [13]. If hard QCD processes contribute to the  $\langle \cos\phi \rangle$  or the  $\langle \cos 2\phi \rangle$ , one would



expect these moments to show a dependence on the  $p_T$  of the trigger particle. However, no such variation is seen for either moment as shown in fig. 4b. This again indicates that hard QCD processes are not the dominant source of the large negative  $\langle \cos\phi \rangle$  observed at positive  $x_F$  (fig. 3).

Higher twist effects such as those calculated by Berger [3] have a  $1/Q^2$  dependence and should be more significant at low  $Q^2$ . Figure 5 shows that there is very little  $Q^2$  or  $W^2$  dependence in  $\langle \cos\phi \rangle$ . From fig. 5 it can also be seen that the asymmetry in  $\langle \cos\phi \rangle$  between negative and positive  $x_F$  is present in all intervals of  $Q^2$  and  $W^2$ .

Figure 6 shows  $\langle \cos 2\phi \rangle / f_2(y)$  and  $\langle \sin\phi \rangle / f_3(y)$  as a function of  $x_F$ . It is clear that  $\langle \sin\phi \rangle$  is zero within statistical errors for all  $x_F$ . The  $\langle \cos 2\phi \rangle$  seems to be small except for a small positive region around an  $x_F \approx 0.3$  consistent with the data in [5].

### Conclusions

A strong dependence of  $\langle \cos\phi \rangle$  on  $x_F$  has been observed with a value dropping below  $-0.1$  in the forward direction and a small and positive value in the backward direction. The general trends of the data are predicted by the model of König and Kroll. However, the amplitude of  $\langle \cos\phi \rangle$  at positive  $x_F$  and its rapid change at  $x_F$  close to 0 are not reproduced by the model. Variations of the parameters of the model indicate that hard QCD processes contribute only a small amount to the non-zero  $\langle \cos\phi \rangle$ , while a value of  $\langle K_T^2 \rangle \geq (0.44 \text{ GeV})^2$  was indicated for the intrinsic  $K_T$  of the struck quark. The relatively minor contribution of hard QCD processes to the non-zero  $\langle \cos\phi \rangle$  was also suggested by studies of  $\langle \cos\phi \rangle$  as a function of  $p_T$ . The values of  $\langle \cos 2\phi \rangle$  and  $\langle \sin\phi \rangle$  were found to be close to zero although there is an indication that  $\langle \cos 2\phi \rangle$  becomes positive at an  $x_F \approx 0.3$ .

### Acknowledgements

We wish to thank all the people in the various laboratories who have contributed to the construction, operation and analysis of this experiment. The support of the CERN staff in operating the SPS, the muon beam and computer facilities is gratefully acknowledged.

### References

- [1] H. Georgi and H.D. Politzer Phys. Rev. Lett. 40 (1978) 3.
- [2] R.N. Cahn, Phys. Lett. 78B (1978) 269.
- [3] E.L. Berger, Z. Phys. C4 (1980) 289.
- [4] A. König and P. Kroll, Z. Phys. C16 (1982) 891, 445.
- [5] EMC, J.J. Aubert et al., Phys. Lett. 130B (1983) 118.
- [6] A. Mendez et al., Nucl. Phys. B148 (1979) 499.
- [7] E. Berger and P. Kroll, private communication.
- [8] EMC, O.C. Allkofer et al., Nucl. Inst. and Meths. 179 (1981) 445.  
EMC, J.P. Albanese et al., Nucl. Inst. and Meths. 212 (1983) 111.  
EMC, J.P. Albanese et al., Phys. Lett 144B (1984) 302.
- [9] A. Johnson, Ph.D. Thesis, University of Oxford, England (1983).
- [10] G. Ingleman et al., Nucl. Phys. B206 (1982) 239.  
B. Andersson et al., Phys. Rep. 97 (1983) 31.
- [11] EMC, M. Arneodo et al., Phys. Lett. 149B (1984) 415.
- [12] EMC, J.J. Aubert et al., Z. Phys. C30 (1986) 23.
- [13] EMC, J.J. Aubert et al., Phys. Lett. 100B (1981) 433.  
M. Düren, Diplom Thesis, University of Aachen (1981).

Figure Captions

- Fig. 1 Definition of the kinematic variables  $K_T$ ,  $p_T$  and  $\phi$ .  
Adapted from a figure of Mendez et al., [6].
- Fig. 2  $\phi$  distributions of charged hadrons in four  $x_F$  regions for  $p_T > 0.2$  GeV. The curves show the results of the fits.
- Fig. 3  $\langle \cos\phi \rangle / f_1(y)$  as a function of  $x_F$  for charged hadrons with  $p_T > 0.2$  GeV. In addition points are shown from reference [5]. The curves show the predictions of the model of ref. [4].
- Fig. 4a  $\langle \cos\phi \rangle / f_1(y)$  for charged hadrons as a function of the cut (lower bound) applied in  $p_T$ . Four different  $x_F$  regions are shown.
- b  $\langle \cos\phi \rangle / f_1(y)$  and  $\langle \cos 2\phi \rangle / f_2(y)$  as a function of the  $p_T$  of the trigger particle used to select the event.
- Fig. 5  $\langle \cos\phi \rangle / f_1(y)$  of charged hadrons with  $p_T > 0.2$  GeV as a function of  $x_F$  for various regions of (a)  $Q^2$  and (b)  $W^2$  (in  $\text{GeV}^2$ ).
- Fig. 6  $\langle \cos 2\phi \rangle / f_2(y)$  and  $\langle \sin\phi \rangle / f_3(y)$  as a function of  $x_F$  for charged hadrons with  $p_T > 0.2$  GeV.

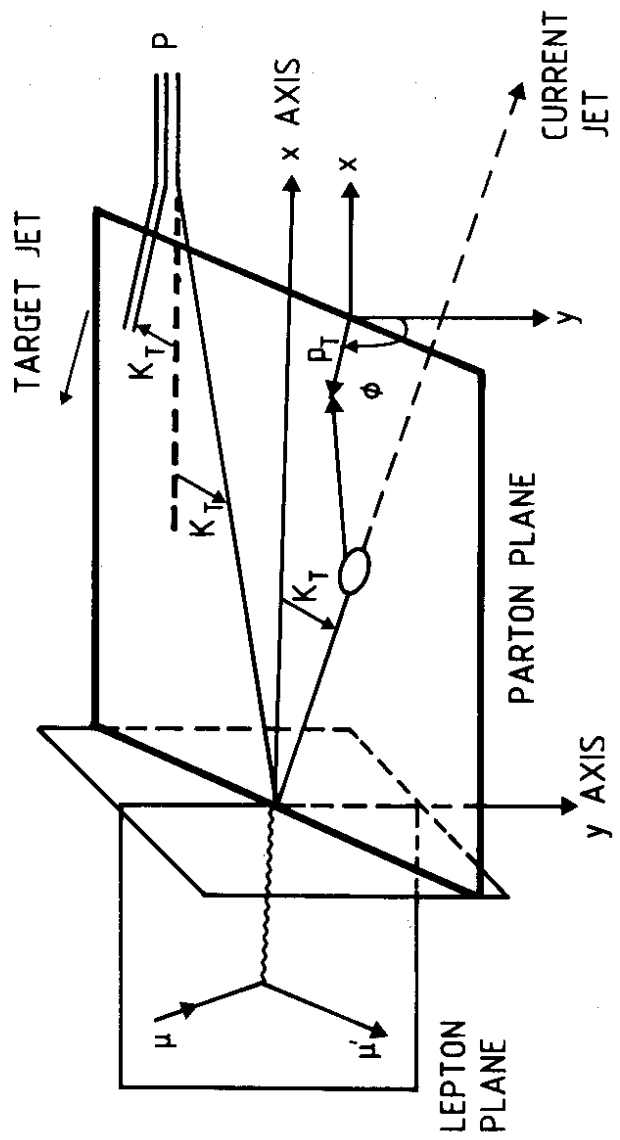


FIG. 1

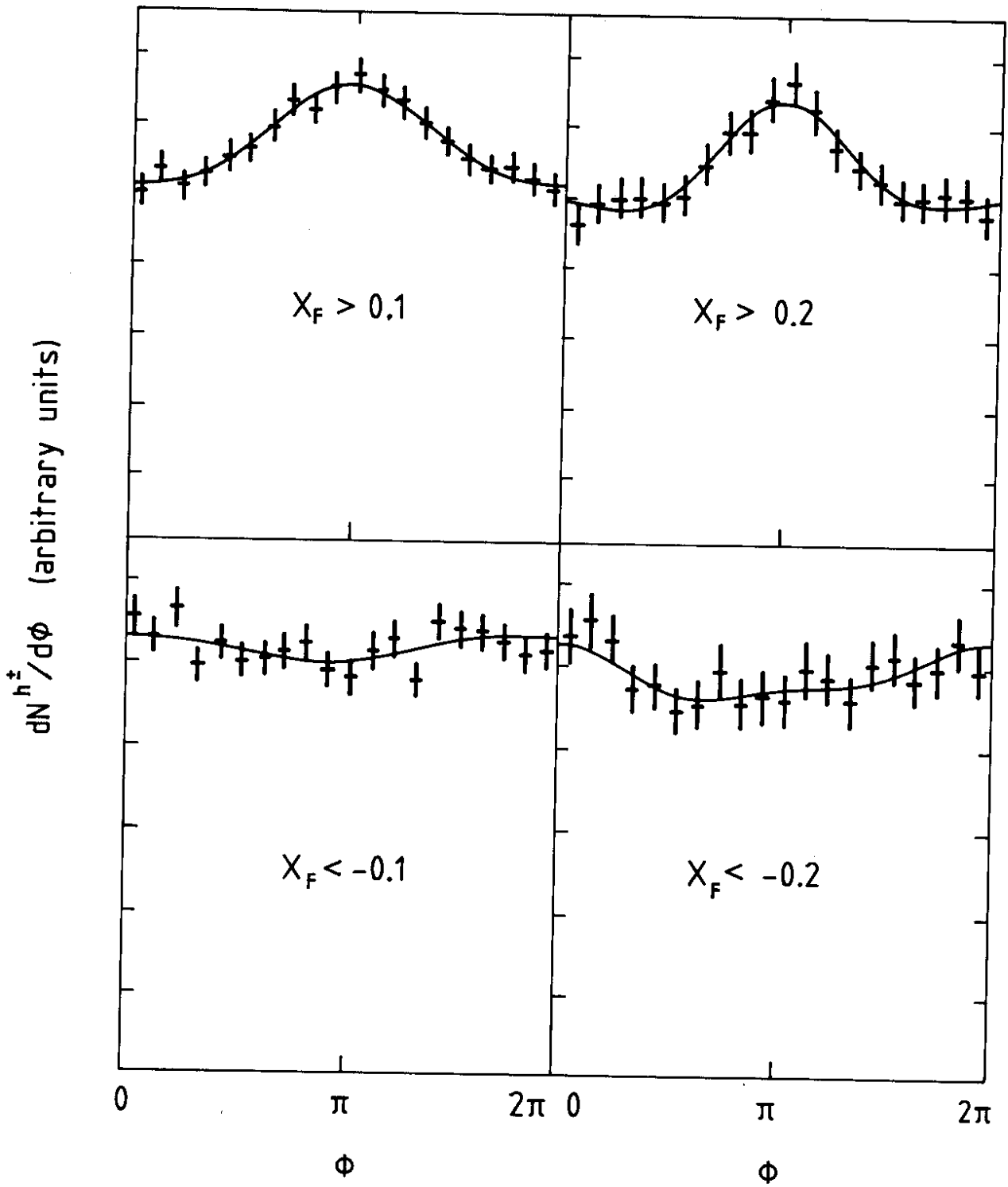


FIG. 2

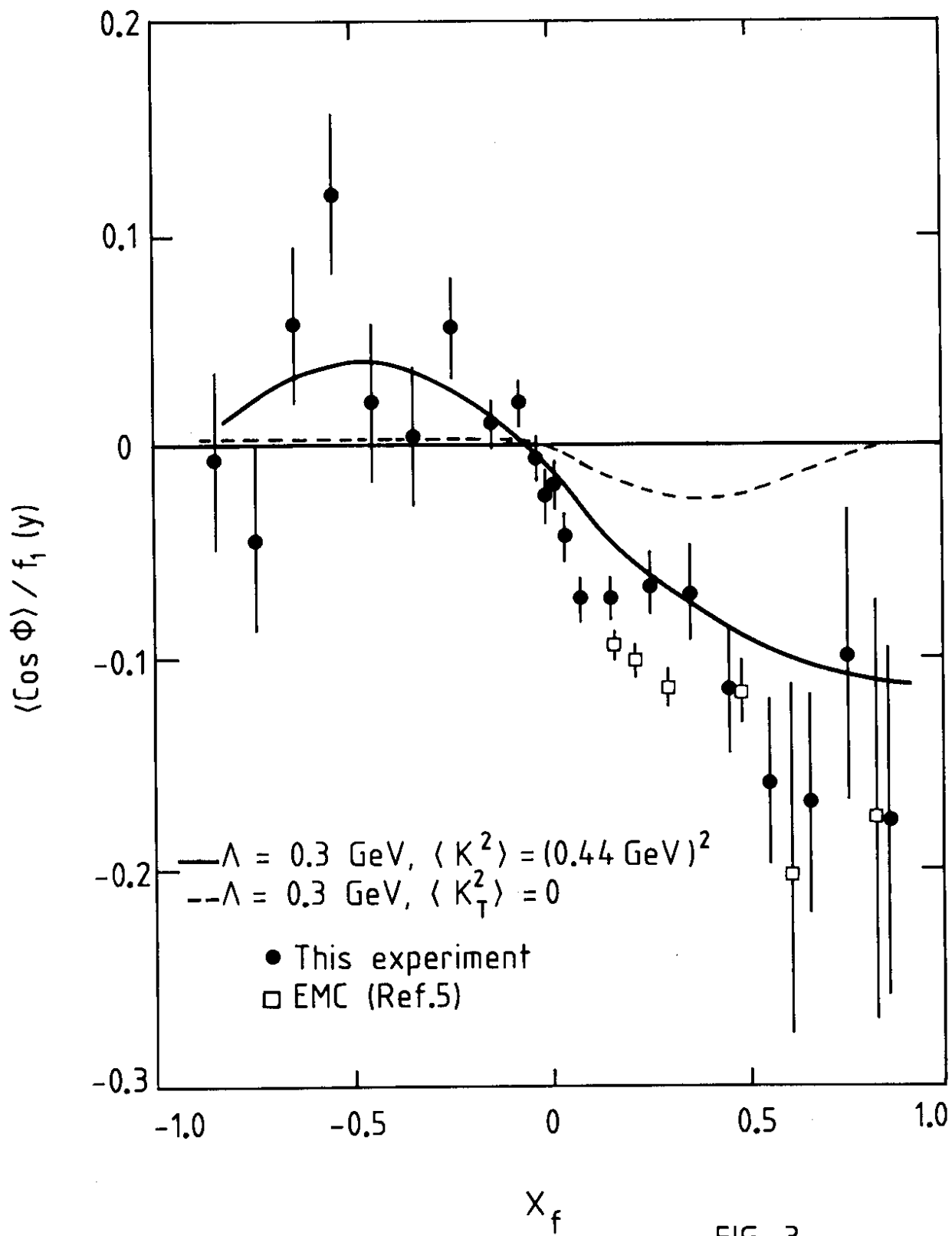


FIG. 3

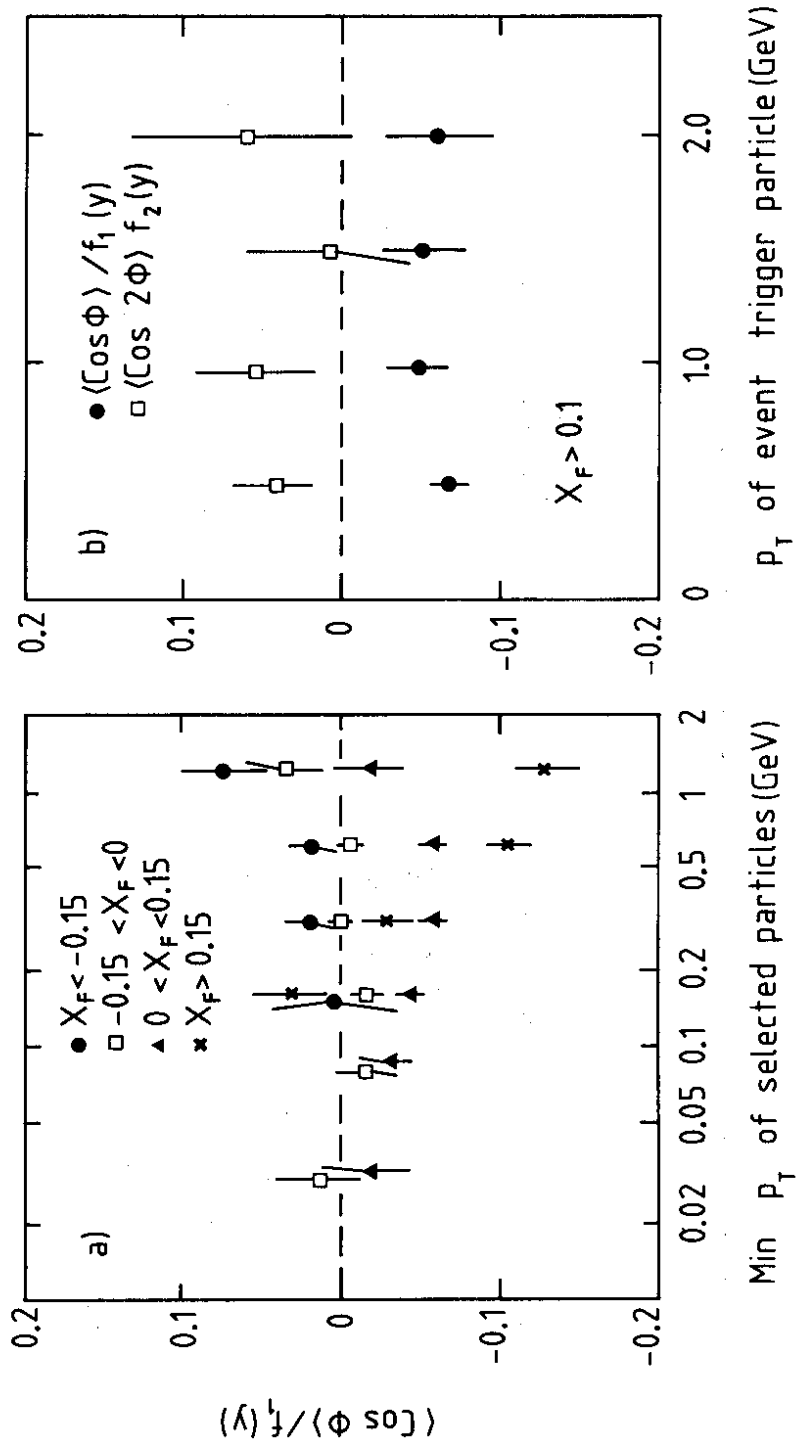


FIG. 4

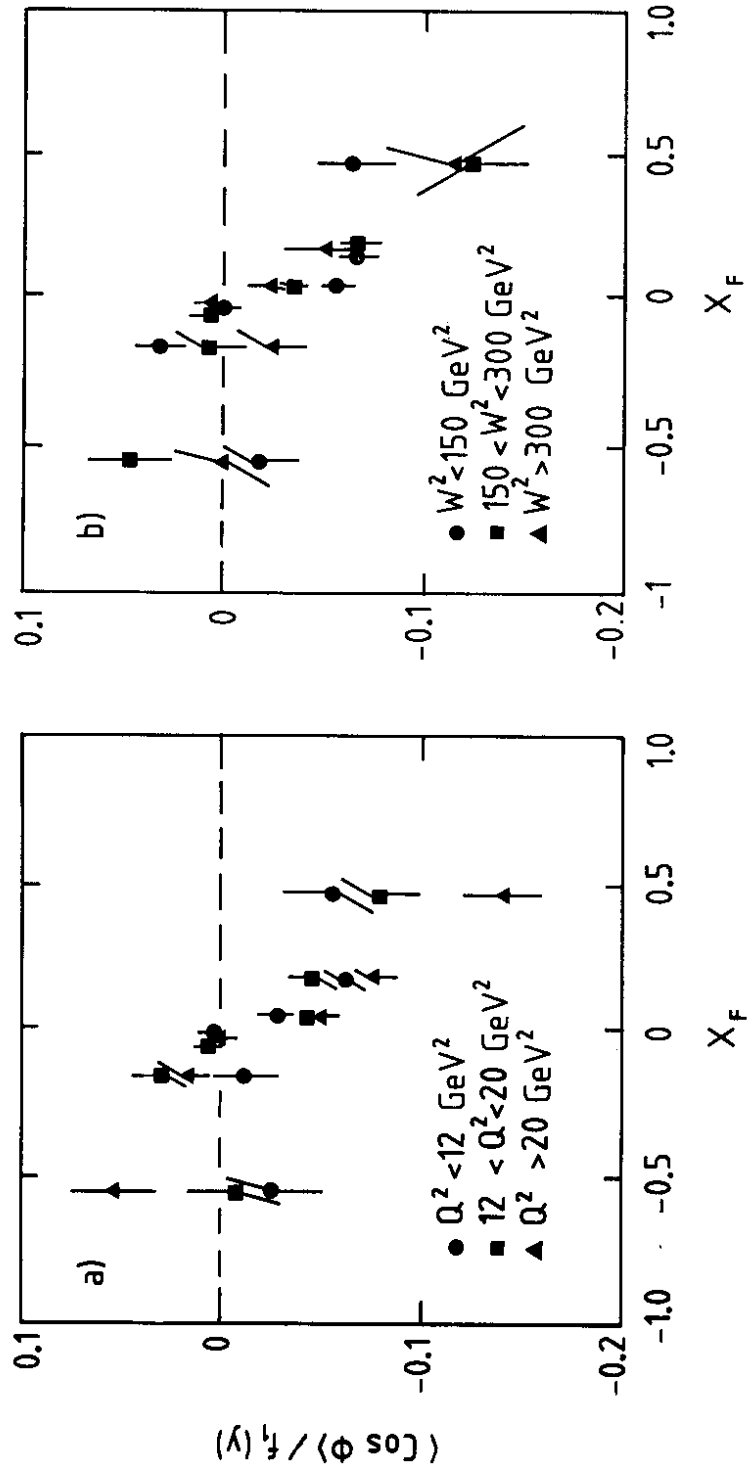


FIG. 5



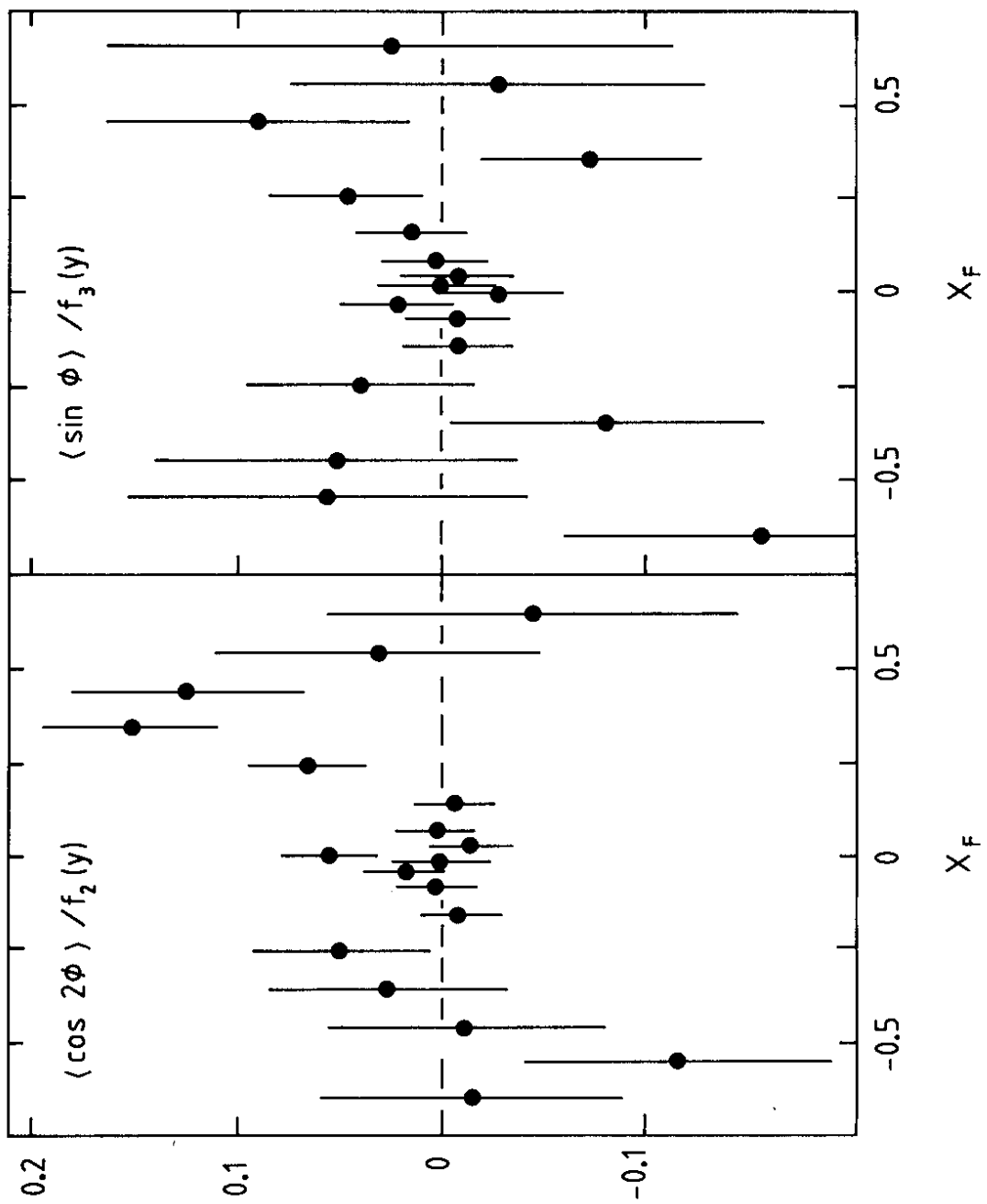


FIG. 6